Heat Loss and Neutron Economy Analysis for Heavy Water Reactor Lattice without Insulating Calandria Tube

Faruk Celik [a], Douglas A. Fynan [a*]
[a]*Ulsan National Institute of Science & Technology, School of Mechanical, Aerospace & Nuclear Engineering, UNIST-gil 50, Eonyang-eup, Ulju-gun Ulsan, 44919, Rep. of Korea*
[*]*Corresponding author: dfynan@unist.ac.kr*

1. Introduction

Most heavy water power reactors (HWRs) are the pressure-tube type where the fuel channels and high-temperature coolant are separated from the low-pressure and low-temperature heavy water moderator by a pressure-retaining boundary (the pressure tube). Heat loss from the channel to moderator is minimized by an insulating gas annulus (usually CO_2) between the pressure tube (PT) and calandria tube (CT). However, approximately 5% of the fission reaction Q-value is still lost to the moderator, primarily through neutron and gamma heating, and this heat is rejected through the moderator cooling system. Only in pressure-vessel type HWRs (Agesta, MZFR, Atucha-I, Atucha-II) can the neutron and gamma heating of the moderator be converted to useable energy by maintaining the moderator temperature above 200 °C and rejecting heat to the feedwater heaters.

This study reassesses the effectiveness of the CT and annulus gas system (AGS) of the CANDU-6 HWR from energy balance and neutron economy perspectives and considers the removal of these structures and systems. The following engineering, radiological, and safety considerations motivated the study. All in-core structures are parasitic absorbers of neutrons negatively affecting neutron economy. The reactivity worth of calandria tubes in the CANDU lattice is approximately -9 mk. All in-core zirconium alloys become activated with long-lived ^{93}Zr (1.5×10^6 year half-life), so the calandria tubes become high-level waste after plant decommissioning. Reactors that have larger inventories of zirconium such as boiling water reactors with Zircaloy wrapper boxes and CANDUs with PTs and CTs produce more hydrogen (or deuterium) gas during severe accidents. The AGS and supporting subsystems adds to the complexity of the plant. Production of activation product ^{14}C in the AGS contributes to the release of radioactive effluent from CANDU reactors [1]. Leakage of CO_2 into the moderator has caused rapid precipitation of moderator soluble poison that if went undetected would have resulted in the loss of guaranteed shutdown state [2,3].

In Section 2, a model for calculating heat loss from a CANDU-6 fuel channel with and without the CT is presented. A parametric study of heat loss for high, low, and average channel powers and different combinations of moderator temperature (T_m) and moderator velocity (v_m) establishes moderator heating only increases by a factor of two for a lattice without CTs in Section 3. In Section 4, lattice criticality and burnup simulations with a Monte Carlo code finds the optimal lattice pitch for a channel without CT is 26.422 cm, over 2 cm less than the CANDU-6 lattice pitch, allowing for either a 380-channel core to be constructed with significant heavy water savings or a 460-channel core with same heavy water inventory as the CANDU-6 resulting in net power uprate of the plant despite the increased heat loss. The optimized lattice pitch has improved neutron economy resulting in increased discharge burnup which compensates for the additional heat loss from a fuel-cost perspective.

2. Fuel Channel Heat Loss Model

The thermal-hydraulic (TH) analysis of the fuel channel and heat loss is performed with coupled one-dimensional TH solver for coolant flow and temperature distribution in the channel and radial heat conduction model for heat transfer to the moderator. For an assumed channel power, the steady-state coolant mass flow rate ($\dot{m}$) that satisfies a desired coolant outlet temperature (310 °C) is solved using finite differencing solution of the control volume approach through iterative Gauss-Seidel update of an initial value problem (IVP) from an initial guess of the coolant mass flow rate and known inlet coolant temperature (T_0 = 266 °C). The radial temperature profile through the channel structures is obtained simultaneously by solving the one-dimensional radial heat conduction equation with moderator temperature (T_m) and local moderator velocity boundary conditions (BCs) applied at the CT (or PT) boundary with the moderator. Fig. 1 shows a control volume segment along the channel. Table I lists geometric and thermal hydraulic parameters used in the calculations.

2.1. Coolant Temperature Profile

The governing equation for one-dimensional steady-state energy balance for the channel is the change of coolant temperature (T) per unit length of channel which is equal to the rate of energy transferred from the fuel to coolant and the heat loss through the pressure tube wall

$$\dot{m}c_p\frac{dT}{dx} = \dot{q}(x) + 2\pi(T_m - T)/\Omega \ , \quad (1)$$

where $\dot{q}$ is the linear heat generation rate of the fuel bundle. The thermal resistance Ω of the CANDU-6 lattice with structure thermal conductivities (k_{pt}, k_{ct}, k_{gap}) is

$$\Omega = \frac{1}{r_1 h_c} + \frac{\ln\left(\frac{r_2}{r_1}\right)}{k_{pt}} + \frac{\ln\left(\frac{r_3}{r_2}\right)}{k_{gap}} + \frac{\ln\left(\frac{r_4}{r_3}\right)}{k_{ct}} + \frac{1}{r_4 h_m} \quad . \qquad (2a)$$

For an uninsulated channel with the CT and annular gas removed, the PT and convective inner and outer wall surfaces are the thermal resistance

$$\Omega = \frac{1}{r_1 h_c} + \frac{\ln\left(\frac{r_2}{r_1}\right)}{k_{pt}} + \frac{1}{r_2 h_m} \quad . \qquad (2b)$$

The heat loss to the moderator is proportional to the temperature differential between the coolant and moderator.

Integrating Eq. 1 over a control volume segment with $\Delta x = x_n - x_{n-1}$ gives the energy balance for the control volume

$$\int_{x_{n-1}}^{x} \dot{m} c_p dT = \int_{x_{n-1}}^{x} [\dot{q}(x) + 2\pi(T_m - T)/\Omega] dx$$

$$\dot{m} c_p (T_n - T_{n-1}) = q + 2\pi(T_m - \bar{T}_n)/\Omega \quad , \qquad (3)$$

with q as the fraction of the bundle power in node n. The average coolant temperature in node n is defined as

$$\bar{T}_n = \int_{x_{n-1}}^{x} T(x) dx / \Delta x \; . \qquad (4a)$$

In the finite differencing solution Eq. 4a is approximated as the simple average of the coolant temperatures at the control volume boundaries

$$\bar{T}_n = T_n + T_{n-1}/2 \; . \qquad (4b)$$

In the control volume, the coolant properties density (ρ), specific heat capacity (c_p) thermal conductivity (k), and dynamic viscosity (μ) are calculated at the average coolant temperature. The axial coolant temperature profile is solved by finite differencing IVP

$$T_n^{j+1} = T_{n-1}^{j} + \frac{1}{\dot{m} c_p}\left(q - 2\pi\Delta x\left(\bar{T}_n^{j} - T_m\right)/\Omega\right) \; . \qquad (5)$$

From the initialization of control volume temperatures $T_{n-1}^0 = T_n^0 = \bar{T}_n^0$, Eq. 5 is iterated until the average node temperature (from which the heat loss to the moderator is dependent on) converges as $\left|\bar{T}_n^{j+1} - \bar{T}_n^{j}\right| < 10^{-4}$.

2.1.1 Coolant Heat Transfer Coefficient

The coolant flow inside the pressure tube is turbulent internal flow. In the Eqs. 2a and 2b, the convective heat transfer coefficient h_c for heat transfer from the coolant to PT inner wall with radius r_1 is obtained from the Dittus-Boelter correlation [8] using the Nusselt number

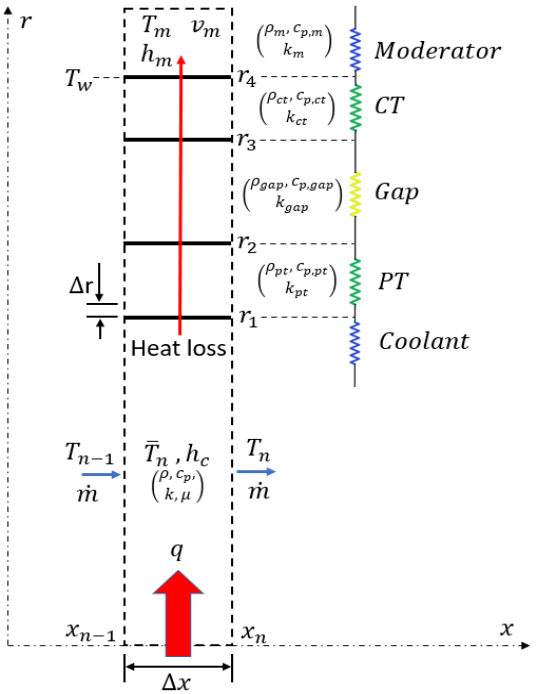

Fig. 1. Control volume of CANDU-6 channel.

$$Nu = \frac{h_c D_h}{k} = 0.023 Re^{0.8} Pr^{0.3} \; . \qquad (6)$$

The Reynolds number $Re = vD_h\rho/\mu$ and Prandtl number $Pr = \mu c_p/k$ are calculated using the thermophysical properties of heavy water calculated at the current node average temperature and using the cooling value (0.3) for the Prandtl number exponent.

2.1.2 Moderator Heat Transfer Coefficient

Inside the calandria vessel, the flow is both natural and forced convection from buoyancy forces and moderator cooling system circulation [4]. The heat transfer coefficient (h_m) for heat transfer to the moderator is derived from the total Nusselt number of the mixed convection flow [9] as

$$Nu_m = \frac{h_m D_h}{k} = \left(Nu_{free}{}^3 + Nu_{force}{}^3\right)^{\frac{1}{3}} . \qquad (7)$$

Natural convection is based on the Raleigh number

$$Ra = \frac{g\beta(T_w - T_m) L_c^3 \rho^2 c_p}{\mu k} \; , \qquad (8)$$

which is a function of wall outer surface temperature T_w and moderator temperature. The wall temperature is the outer surface temperature of the CT for the insulated case and the outer surface temperature of the PT in the uninsulated case. The characteristic length L_c is chosen as the hydraulic diameter D_h (the wetted perimeter of the CT or PT) in this problem.

The Churchill-Chu correlation which has a restriction of $Ra < 10^{12}$ [10] is used to calculate the moderator free convective Nusselt number

$$Nu_{free} = \left(0.6 + \frac{0.387 Ra^{\frac{1}{6}}}{\left[1 + \left(\frac{0.559}{Pr}\right)^{\frac{9}{16}}\right]^{\frac{8}{27}}} \right)^2 . \quad (9)$$

The Churchill-Bernstein correlation [11] proposed a single representative forced convection correlation which can cover all range of Re as

$$Nu_{force} = 0.3 + \frac{0.62 Re^{\frac{1}{2}} Pr^{\frac{1}{3}}}{\left[1 + \left(\frac{0.4}{Pr}\right)^{\frac{2}{3}}\right]^{\frac{1}{4}}} \left[1 + \left(\frac{Re}{282000}\right)^{\frac{1}{2}}\right]. \quad (10)$$

2.2. Gauss-Seidel Update of The Wall Temperature

The heat transfer coefficient of the moderator is a function of outer surface temperature of the wall resulting in a recursive relationship between heat loss, radial temperature profile, and heat transfer coefficient. The recursive problem is solved using the one-dimensional unsteady-state heat conduction governing equation for radial temperature profile (T_r) across the channel structures

$$\frac{\partial T_r}{\partial t} = a\left(\frac{1}{r}\frac{\partial T_r}{\partial r} + \frac{\partial^2 T_r}{\partial r^2}\right), \quad (11)$$

where $a = k/\rho c_p$ stands for the thermal diffusivity of the wall material. Based on the finite difference method, $\partial T_r/\partial r$ and $\partial^2 T_r/\partial r^2$ are converted to central difference scheme while $\partial T_r/\partial t$ can be approximated by first-order time forward difference. The final model that is applied to the radial mesh (indexed by k with K meshes) in the interior of the structure is

$$T_{r,k}^i = \alpha T_{r,k-1}^{i+1} + \varphi T_{r,k}^{i+1} + \gamma T_{r,k+1}^{i+1} . \quad (12)$$

The coefficients $(\alpha, \varphi, \gamma)$ of the model are $(a\Delta t/2r\Delta r - a\Delta t/\Delta r^2)$, $(1 + 2a\Delta t/\Delta r^2)$, and $(-a\Delta t/2r\Delta r - a\Delta t/\Delta r^2)$, respectively. At r_1, and either r_2 or r_4, the model has internal and external BCs which are coolant convection and moderator convection, respectively. The equations of $-k\partial T_r/\partial r = h_c[\bar{T}_n - T_{r=r_1}]$ (coolant) and $-k\partial T_r/\partial r = h_m[T_w - T_m]$ (moderator) where $T_w = T_{r=r2,r4}$ are used to solve the boundary value problems

$$T_{r,0}^{i+1} = T_{r,2}^{i+1} - \frac{1}{b}T_{r,1}^{i+1} + \frac{1}{b}\bar{T}_n \quad and \quad (13a)$$

$$T_{r,K}^{i+1} = T_{r,K-2}^{i+1} - cT_{r,K-1}^{i+1} + cT_m . \quad (13b)$$

Table I. CANDU-6 Lattice Properties [4,5,6,7]

Parameter	Unit	Value
Thermal Power per Channel	MW	3.0/5.4/6.8
Coolant Inlet Temperature	°C	266
Coolant Outlet Temperature	°C	310
Coolant & Moderator	-	D_2O
Coolant Pressure	MPa	10.5
Moderator Temperature	°C	40-90
Moderator Pressure	atm	1
Moderator Flow Velocity	m/s	0.01/0.1/0.5
No. of Bundles per Channel	-	12
No. of elements per Bundle	-	37
Annular Gap	-	CO_2
Annular Gap Temperature	°C	167
Annular Gap Pressure	atm	1
Pressure & Calandria Tube	-	Zircaloy-2
Inner Radius of PT (r_1)	cm	5.20
Outer Radius of PT (r_2)	cm	5.60
Inner Radius of CT (r_3)	cm	6.46
Outer Radius of CT (r_4)	cm	6.60
Outer Radius of Cladding	cm	0.65

The coefficients b and c are $k/2\Delta r h_c$ and $2\Delta r h_m/k$, respectively. Combing Eqs. 12, 13a, and 13b, give finite differencing solutions at the boundaries as

$$bT_{r,1}^i - \alpha\bar{T}_n = (\varphi b - \alpha)T_{r,1}^{i+1} + (\alpha b + \gamma b)T_{r,2}^{i+1} \quad (14a)$$

$$T_{r,K-1}^i - \gamma d T_m = (\alpha + \gamma)T_{r,K-2}^{i+1} + (\varphi - \gamma d)T_{r,K-1}^{i+1} \quad (14b)$$

The radial mesh temperatures (Eqs. 12, 14a, and 14b) are represented in matric form as $Ax = B$:

$$A = \begin{bmatrix} \varphi_{r,1}b_{r,1} - \alpha_{r,1} & \alpha_{r,1}b_{r,1} + \gamma_{r,1}b_{r,1} & 0 \ \dots \\ \alpha_{r,2} & \varphi_{r,2} & \gamma_{r,2}\cdots \\ \vdots & \vdots & \vdots \\ \dots \alpha_{r,k} & \varphi_{r,k} & \gamma_{r,k}\dots \\ \vdots & \vdots & \vdots \\ \cdots \alpha_{r,K-2} & \varphi_{r,K-2} & \gamma_{r,K-2} \\ \cdots 0 & \alpha_{r,K-1} + \gamma_{r,K-1} & \varphi_{r,K-1} - \gamma_{r,K-1}c_{r,K-1} \end{bmatrix}$$

$$x = \begin{bmatrix} T_{r,1}^{i+1} \\ T_{r,2}^{i+1} \\ \vdots \\ T_{r,k}^{i+1} \\ \vdots \\ T_{r,K-2}^{i+1} \\ T_{r,K-1}^{i+1} \end{bmatrix}, B = \begin{bmatrix} b_{r,1}T_{r,1}^i - \alpha_{r,1}\bar{T}_n \\ T_{r,2}^i \\ \vdots \\ T_{r,k}^i \\ \vdots \\ T_{r,K-2}^i \\ T_{r,K-1}^i - \gamma_{r,K-1}c_{r,K-1}T_m \end{bmatrix}. \quad (15)$$

The models for coolant axial and radial temperature profiles are solved using Gauss-Seidel numerical method as an iteration method. Based on this numerical method, a Matlab code was developed. The radial meshing thickness Δr is set from 16 evenly spaced mesh grids in the PT region, 5 in CO_2, and 5 in the CT. The axial coolant control volume nodalization divides the 12 fuel bundles into N=200 evenly spaced segments of length Δx . A radial temperature profile calculation takes

approximately 6000 time-step iterations of the unsteady transient model to converge to steady-state radial temperature profile with convergence criterion $\left|T_{r,k}^{i+1} - T_{r,k}^{i+1}\right| < 10^{-4}$. To initialize the transient problem, the outer wall surface temperature is set to $T_{r,K}^{0} = 100\ °C$ which is above the maximum moderator temperature range and below the coolant inlet temperature.

The analysis code starts with initial coolant mass flow rate guess $\dot{m}^{z} = \dot{m}^{0}$ in Eq. 5. After the inner iterations of coolant temperature and radial temperature distributions are converged, the coolant outlet temperature predicted by the TH solver is compared to the target (310 °C). Outer sweeps and iterative update of $\dot{m}^{z} \rightarrow \dot{m}^{z+1}$ are preformed until convergence

$$\left|T_{N}^{i+1}|_{\dot{m}^{z+1}} - 310\ °C\right| < 0.1\ °C\ . \qquad (16)$$

The total heat loss is summed from the heat losses from each control volume.

In an actual operating CANDU calandria, the moderator temperature and flow velocities follow complex three-dimensional distributions which have been predicted by computational fluid dynamics [4], and each fuel channel has a unique axial power distribution that evolves continually in time. The preceding numerical model is general such that if the local moderator conditions around a particular fuel channel and axial power distribution are known, these BCs can be implemented in vector form for the control volume segments. The proceeding heat loss calculations aim to establish realistic "typical" or "average" heat loss values which can inform conceptual design changes to the CANDU-6 lattice, so average and bounding values are applied in the parametric study. High moderator velocities (~0.5 m/s) which enhance heat loss, occur locally around the moderator inlet jets near some low-power channels at the core periphery [4]. The 0.5 m/s cases are absolute upper bound estimates of heat loss.

3. Heat Loss Results

Figure 2 shows the heat loss results for CANDU-6 lattice with the insulating gas annulus and CT. The heat loss is insensitive to channel power and is less than half of a percent of the channel power due to the insulating gas annulus. The moderator velocity changes the heat transfer coefficient and thermal resistance at the CT outer wall, but the heat loss only varies between 5% to 10% over the whole range of moderator velocities. Heat loss varies by approximately 20% over range of moderator temperatures.

Figure 3 shows the channel power and mass flow rate relationship. All channel powers have coolant temperature gradient from 266 °C to 310 °C, so heat loss is insensitive to mass flow rate. Coolant velocity only affects heat loss through the heat transfer coefficient at the PT inner wall which is a very small component of the overall thermal resistance (Eq. 2a). Figure 3 actually contains three curves show in the detail in the inset

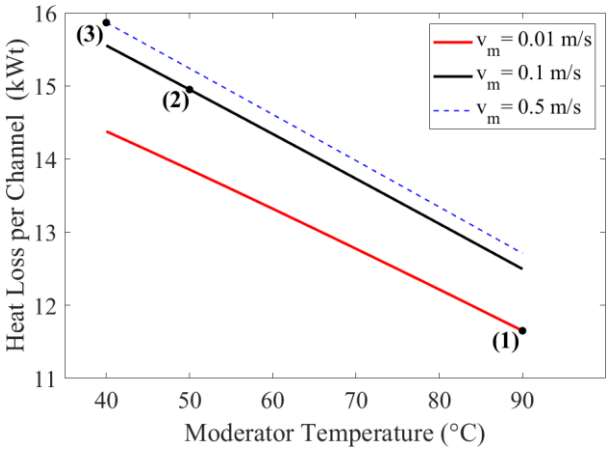

Fig. 2. Heat loss from the 5.4 MWt insulated channel.

corresponding to points 1 – 3 on Fig. 2. Point 1 is the bounding case with moderator temperature and velocity BCs (T_m = 90 °C, v_m = 0.01 m/s) that yield the minimum heat loss. Point 2 represents typical moderator operating conditions (T_m= 50 °C, v_m = 0.1 m/s). Point 3 is maximum heat loss bounding case (T_m= 40 °C, v_m = 0.5 m/s). The three curves only show a slight variation in flow rate (~30 g/s) meaning heat loss from an insulated channel has almost no effect on channel flow rate and coolant energy balance.

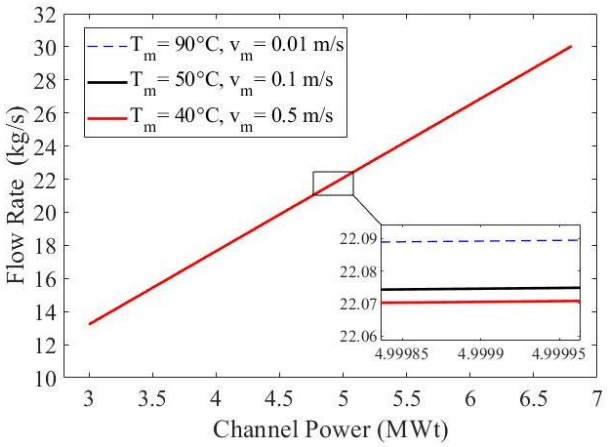

Fig. 3. The coolant flow rates for insulated channel as a function of channel power.

Figure 4 shows the heat loss from the uninsulated channel. From Eq. 2b, the heat transfer coefficient of the PT outer wall is the dominate parameter of the thermal resistance, so heat loss is a strong function of the moderator velocity. Included in Fig. 4 are curves for 0.2 m/s moderator velocity because the moderator cooling system flow rate and therefore the average moderator velocity will likely have to be doubled to accommodate the additional heat loss. For a given moderator velocity, the high-power channel has the largest heat loss because higher coolant velocity enhances heat transfer at the PT inner wall and reduces the overall thermal resistance. On a percentage basis, heat loss could be as high as 24% for a low-power channel but the typical range is between 5%

to 10%. If a core is to be built and operated without CTs, emphasis should be put on flux flattening (e.g., use adjustor rods) because the low-power channels have the highest heat loss percentages. Secondly, the operating conditions of the moderator cooling system should be optimized to minimize heat loss either from higher average moderator temperature or larger enthalpy rise of the moderator thereby reducing flow rate and average moderator velocity.

Figure 5 shows the channel flow rates as a function of channel power and heat loss. For constant channel power, the channel flow rate is a function of the heat loss sensitivity to heat transfer at the PT outer wall but is insensitive to moderator temperature due to a cancelation of two effects with feedback. Increasing moderator temperature decreases heat loss which means more of the channel power goes to heating the coolant. Coolant flow rate must increase to maintain the constant outlet temperature while increased coolant velocity enhances heat transfer at the PT inner wall. Variation in flow rate (several kg/s) for a given channel power is large enough that an operating channel flow rate may need to be adjusted via flow orifice to maintain desired outlet conditions dependent on the local moderator conditions of that channel.

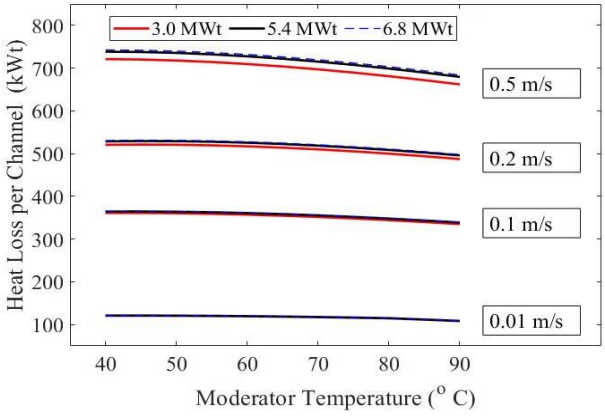

Fig. 4. Heat loss from uninsulated channel.

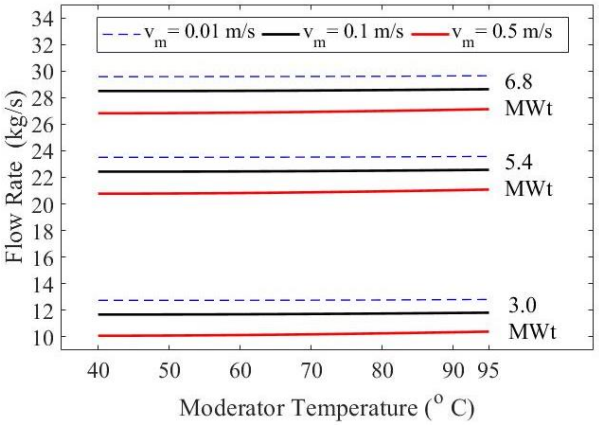

Fig. 5. The coolant flow rate for uninsulated channel as a function of moderator temperature.

The key result from this section is that the heat loss from an uninsulated channel is approximately the same as the heat loss to moderator from gamma and neutron heating. Over 80% of the operated HWRs were designed with this negative attribute of unrecoverable heat to the moderator, despite other design choices, i.e., the pressure-vessel type HWR, so future work should identify the maximum allowable heat loss that can be justified (economically) in a pressure-tube type HWR and if the actual heat loss from an uninsulated channel design falls below this threshold. The next section explores the benefits of CT elimination from the neutron economy and fuel cycle cost perspectives which need to be considered in the economic analyses.

4. Optimal Lattice Pitch of Uninsulated Channel

This study adapts a unit cell model of the CANDU-6 lattice and standard 37-element fuel bundle [5] for infinite-lattice criticality calculations and depletion with the UNIST Monte Carlo MCS [12]. This model and simulations are used to identify the optimal lattice pitch of the uninsulated channel with respect to lattice reactivity (k_∞) and discharge burnup. Figure 6 shows the two-unit cell geometries for the CANDU-6 lattice and uninsulated channel with CT and gas annulus removed. Reflecting BCs are applied on the moderator box surfaces and the coolant gap at the bundle ends. For all criticality simulations, 50 inactive cycles, 250 active cycles, and 50,000 histories per cycle are used which yield statistical standard deviations less than 14 pcm for k_∞ and all power tallies relative standard deviations are less than 1%. For depletion calculations, the bundle power is set to 450 kWt (approximate average bundle power in CANDU-6).

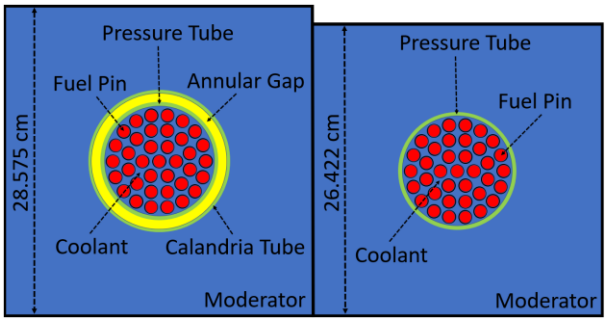

Fig. 6. Cross section views of CANDU-6 lattice and optimized uninsulated channel.

4.1. Lattice Reactivity with Burnup

Figure 7 shows the lattice reactivity of different lattice designs as a function of burnup. For the CANDU-6 reference case, k_∞ at beginning-of-cycle (BOC) is 1.12040. The infinite-lattice depletion calculation shows the ^{135}Xe buildup and the plutonium peak at approximately 1 MWD/kgHM burnup. The k_∞ at end-of-cycle (EOC) is 0.98140 at an assumed discharge burnup

of 7.5 MWD/kgHM which is representative of average discharge burnup of a CANDU-6 with adjustor rods and fueled with natural uranium and 37-element bundle. Performance of lattice designs without CT are assessed relative to these metrics from the reference simulation.

A parametric study of lattice pitch for lattices without CT was performed to identify new pitches that preserve certain properties of the reference lattice. First preserving the CANDU-6 lattice pitch of 28.575 cm results in increased lattice reactivity at BOC (k_∞ = 1.13370) for the new lattice without CT. The discharge burnup of 7.9 MWD/kgHM equals the reference k_∞ at EOC, an increase of 5.3% showing the improved neutron economy of lattice.

Second, the lattice pitch was iterated to find the pitch (26.422 cm) that preserved the reference k_∞ at BOC. Interestingly, this pitch reactivity diverges from the reference after the plutonium peak. Decreasing lattice pitch has subtle influence on the thermal and epithermal neutron spectrum by hardening the spectrum. When ^{239}Pu is present in the fuel, small spectrum hardening increases reactivity due to the resonance at 0.3 eV and increase in the fission-to-capture ratio. As burnup increases, the ^{235}U continues to deplete, and ^{239}Pu (in quasi-equilibrium concentration from continued production from ^{238}U) has increasing relative importance to neutron balance. The discharge burnup for the 26.422 cm pitch is 7.9 MWD/kgHM—the same as the discharge burnup of the 28.575 cm pitch with no CT. This is inspite of the 28.575 cm pitch having significantly higher reactivity at BOC. If burnup is extended past 7.9 MWD/kgHM, the two curves actually cross over. We designate the 26.422 pitch as the "optimal" pitch for uninsulated channel providing increased burnup and significant heavy water savings. From fuel cycle cost perspective, the increased discharge burnup (5.3%) recovers a significant fraction of the additional energy lost to the moderator cooling system as a consequence of eliminating the CT and gas annulus.

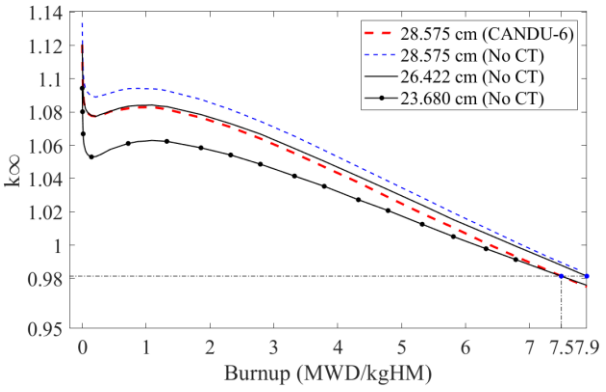

Fig. 7. Lattice reactivity and discharge burnup for different lattice designs.

Finally, the lattice pitch which preserves both discharge burnup and lattice reactivity at EOC was identified to be 23.680 cm. A reactor designed with this much smaller lattice pitch would obviously have significant heavy water savings but with incrementally higher fuel cycle costs (which is generally already very low for natural-uranium HWR fuel cycles). If heavy water cost—which is always large and has varied significantly over the past 70 years due to market conditions and supply/demand dynamics—is a deciding factor in the net present value calculation of a new plant construction study, then both the heavy water savings and fuel cycle costs need to be simultaneously considered in the design optimization.

4.2. Power Uprating and Heavy Water Savings Study

Assuming an optimized pitch of 26.422 cm, Table II summarizes operating data for hypothetical HWR cores that are constructed without CTs. First, a 380-channel core with same power as the CANDU-6 can be constructed with a calandria diameter of 6.30 m, a reduction of 0.46 m relative to the CANDU-6 diameter. Here the thickness of the radial heavy water reflector around the periphery fuel channels is preserved, but the volume of heavy water is significantly reduced. The new 380-channel core is overlain on the CANDU-6 in Fig. 8. Significant heavy water savings is achieved in the outer annulus region of the radial reflector. However, the additional heat loss to the moderator is estimated to be between 129.9 MWt to 195.3 MWt resulting in power downrate (of the net electrical output of the plant) between 6.7% to 10 %, but this downrate is partially compensated by 5.3% increase in discharge burnup. Also, this design with smaller diameter has a higher fuel-to-surface-area ratio which should increase the fast and thermal non-leakage probabilities, so future work needs to consider the increased burnup due to change in leakage at the core reactivity (k_{eff}) level.

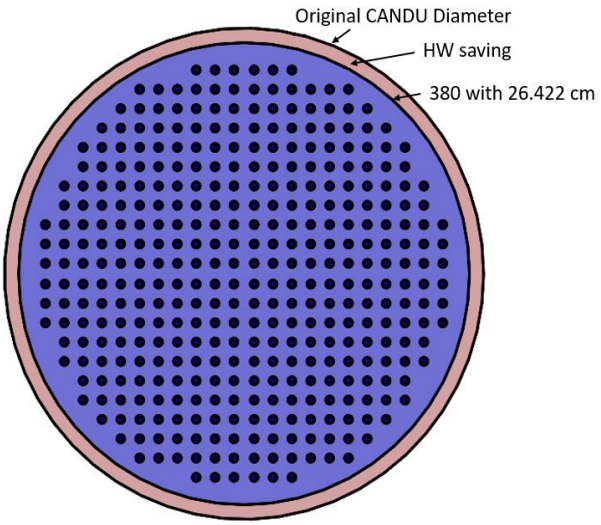

Fig. 8. The calandria tank diameter difference of no CT case.

Table II. Heat Loss, Heavy Water Savings, and Power Uprating Data for HWR Designs without CT

Parameter	Unit	Candu	No CT	
#Fuel Channels	-	380	380	460
Power (3)	MWt	2052	2052	2484
Nuclear HL	MWt	98.7 [3]	~98.7	~119.5
Convective HL(1)	MWt	5.2	135.1	163.5
Convective HL(2)	MWt	5.7	201.0	243.3
Total HL(1)	MWt	103.9	233.8	283.0
Total HL(2)	MWt	104.4	299.7	362.8
C. Tank Dia.	m	6.76	6.30	6.76
Mod. Volume	m^3	184.1	164.6	188.1
Saving	m^3	-	+19.5	-4
Saving	ton	-	+21.5	-4.4

(1) Assuming T_m = 70 °C and v_m = 0.1 m/s
(2) Assuming T_m = 50 °C and v_m = 0.2 m/s
(3) Assuming 5.4 MWt average channel power

A second option, which could be relevant to both existing plants undergoing refurbishment or a new build, is to retain the outer diameter of the CANDU-6 calandria, reflector thickness, and heavy water inventory and add more channels. We estimated the CANDU-6 calandria vessel can accommodate 460 uninsulated channels with 26.422 cm pitch. Despite total heat loss between 283.0 MWt to 362.8 MWt, this core is a net power uprate (in electrical power) of 13% to 9% at the same heavy water cost.

5. Conclusions

Heat loss from uninsulated pressure tubes to the heavy water moderator is the same magnitude as the unavoidable heat loss from nuclear sources (gamma and neutron heating), so elimination of insulating CT and annulus gas system may be feasible in pressure-tube HWRs such as the CANDU-6. Without parasitic CT in-core structures, neutron economy is improved allowing for a decrease in lattice pitch (from 28.575 cm to 26.422 cm) and increased discharge burnup by over 5%, compensating for a significant fraction of the additional heat loss. New cores with the optimized lattice pitch can be designed with either heavy water savings and nominal net electric power downrate relative to the 380-channel CANDU-6 reference, or a net power uprate exceeding 10% by adding more channels (460 total) to a calandria with the same heavy water inventory.

REFERENCES

[1] W. Sohn, D.W. Kang, W.S. Kim, “An Estimate of Carbon-14 Inventory at Wolsong Nuclear Power Plant in the Republic of Korea”, Journal of Nuclear Science and Technology, Vol. 40, No. 8, p. 604-613, August 2003
[2] Canadian Nuclear Safety Commission, “CNSC Staff Integrated Safety Assessment of Canadian Nuclear Power Plants for 2008”, CNSC, August 2009
[3] D.W. Evans, J. Price, D. Swami, E. Fracalanza , M.E. Brett, F.V. Puzzuoli, A. Garg, O. Herrmann, A. Rudolph, C. Stuart, G. Glowa, J. Smee, “Gadolinium Depletion Event in a CANDU Moderator - Causes and Recovery”, Nuclear power plant conference, Canada, 2010.
[4] M. Kim, S.O. Yu, H.J. Kim “Analyses on fluid flow and heat transfer inside Calandria vessel of CANDU-6 using CFD”, Nuclear Engineering and Design, Vol. 236, pp. 1155-1164, 2006.
[5] Y.A. Setiawan, D.A. Fynan “Delayed-Photoneutron Calculator for 37-Element Fuel Bundle in CANDU-6 Lattice”, Korean Nuclear Society Virtual Spring Meeting, May 13-14, South Korea, 2021
[6] W. Peiman, K. Gabriel, I. Pioro, “Thermal Design Options of New Pressure Channel for SCWRs”, ICONE17, July 12-16, Brussels, Belgium, 2009
[7] S. Zhang, W. Wang, Y. Liu, J. Feng, M. Chen “CANDU refueling optimization by successive two-step mathematical programming – I: MILP models for refueling channel selection”, Annals of Nuclear Energy, Vol. 37, pp. 1146–1159, 2010
[8] F.P. Incropera, D. P., Dewitt, T.L. Bergman, A.S. Lavine, “Fundamentals of Heat and Mass Transfer”, John Wiley & Sons, USA, pp. 514, 2006
[9] E. Ruckenstein, R. Rajagopalan, “A Simple Algebraic Method for Obtaining the Heat or Mass Transfer Coefficients Under Mixed Convection”, Chem. Eng. Commun. Vol. 4, pp. 15-39, 1979.
[10] S.W. Churchill, H.H.S. Chu, “Correlating Equations for Laminar and Turbulent Free Convection from a Horizontal Cylinder”, International Journal of Heat Mass Transfer, Vol. 18, pp. 1049-1053, 1974.
[11] S. W. Churchill, M. Bernstein, “A Correlating Equation for Forced Convection from Gases and Liquids to a Circular Cylinder in Crossflow”, Transactions of the ASME Vol. 99, May 1977
[12] H. Lee, W. Kim, P. Zhang, A. Khassenov, Y. Jo, J. Park, J. Yu, M. Lemaire, D. Lee*, “MCS – A Monte Carlo Particle Transport Code for Large-Scale Power Reactor Analysis,” Annals of Nuclear Energy, Vol. 139, pp. 107276, 2020